CFD and Experimental Investigation of the NASA Ames 11-Foot Transonic Wind Tunnel

Veronica Hawke STC
NASA Ames Research Center
Moffett Field, CA 94035
USA

veronica.m.hawke@nasa.gov

John Melton NASA Ames Research Center
NASA Ames Research Center
Moffett Field, CA 94035
USA

john.melton@nasa.gov

Thomas Romer NASA Ames Research Center
NASA Ames Research Center
Moffett Field, CA 94035
USA

thomas.f.romer@nasa.gov

ACKNOWLEDGEMENTS

The authors would like to thank the NASA Ames AA and AOO branches for their ongoing support of this work. We also appreciate the technical expertise and continued help of Michael Schuh, Frank Kmak, and the computational resources provided by the National Aerodynamics Simulator Facility at NASA Ames.

ABSTRACT

Advancements in mesh generation and computational resources now provide the ability to create high-fidelity Computational Fluid Dynamics (CFD) models of the entire test leg of the 11-by 11-foot Transonic Wind Tunnel (TWT). Work began over five years ago to create a detailed Computer Aided Drafting (CAD) model of the 11-ft TWT for use in CFD simulations. Modelling challenges, simulation setup, CFD resource requirements, and initial comparisons with experimental data will be discussed and presented.

The 11-ft TWT is one leg of the Ames Unitary Plan Wind Tunnel (UPWT). Figure 1 below shows an image of the tunnel with the 11-ft TWT circled in green. Further details about the tunnel can be found at the website listed in Reference 1.

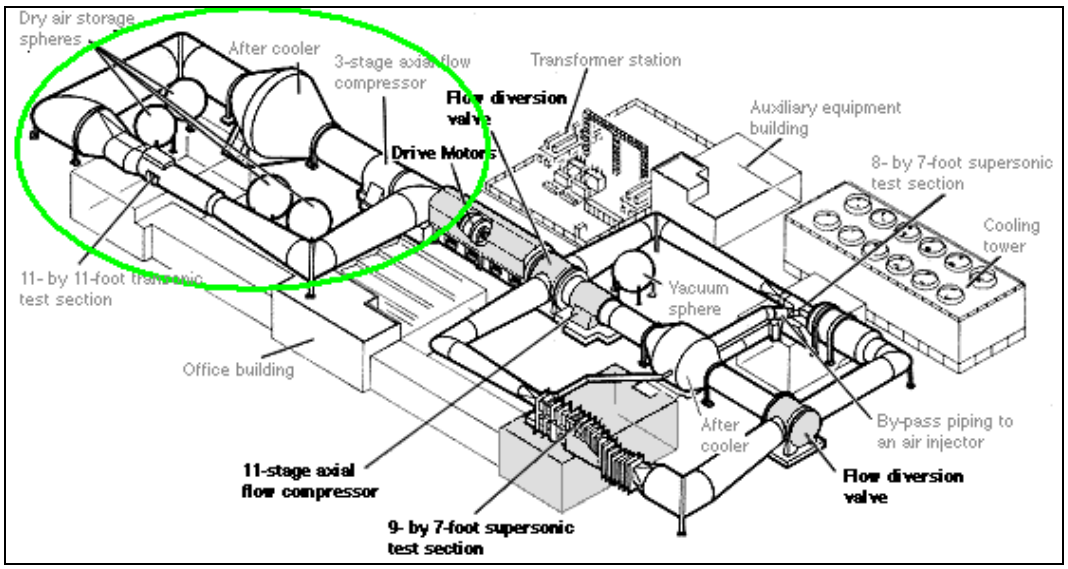

Figure 1: NASA Ames Unitary Plan Wind Tunnel Layout

TABLE OF CONTENTS

Acknowledgements 2
Abstract 2
1.0 Overview 4
2.0 Geometry 4
2.1 Geometry Information Sources 4
2.1 Simulation Geometry 6
2.2 Simulation Description 6
2.3 Simulation Status 7
3.0 Tunnel Testing 7
4.0 CFD Results and Comparisons to Test Data 8
4.1 Target Mach 0.80 9
4.2 Target Mach 1.2 12
5.0 Conclusions 17
References 18

TABLE OF FIGURES

Figure 1 NASA Ames Unitary Plan Wind Tunnel Layout 2
Figure 2 UPWT CAD Model 4
Figure 3 Geometry Modelling Details 5
Figure 4 Coordinate System and Surface Region Layout 5
Figure 5 Partial View of Tunnel Geometry, Surface Mesh and Volume Grid 6
Figure 6 Sample CFD Simulation on 11-ft TWT Strut and Centerbody 7
Figure 7 Sample Simulation Monitor Screen 7
Figure 8 Location of Test Instrumentation for CFD Validation Tests 8
Figure 9 Mach 0.80 Centerline Mach Number 10
Figure 10 Mach 0.80 Boundary Layer Rake Pressures 10
Figure 11 Mach 0.80 Test Section Wall Static Pressure Distribution 11
Figure 12 Aft Diffuser Floor and Wall Static Pressure Distributions 11
Figure 13 Static Pressure Distributions For Aft Diffuser Strut Pressure Trays 12
Figure 14 Mach 0.80 Flow from Upper Plenum Chamber in to Test Section 12
Figure 15 Mach 1.2 Tunnel Centerline Mach Number 13
Figure 16 Mach 1.2 Test Section Boundary Layer Rake Pressures 13
Figure 17 Mach 1.2 Test Section Wall Pressure Distributions 14
Figure 18 Mach 1.2 Aft Diffuser Pressure Distributions 14
Figure 19 Aft Diffuser Strut Pressure Distributions 15
Figure 20 Mach 1.2 Constant Y = 21 Slice 15
Figure 21 Mach 1.2 Flow Through Vortex Generators 16
Figure 22 Flow Through Slot Channels at Forward Test Section 16
Figure 23 Volume Grid for Slot Channels at Forward Test Section 17

1.0 OVERVIEW

Many of NASA's premiere wind tunnel testing facilities were initially constructed in the 1940s and 50s, and have been the subject of numerous modifications and improvements over the intervening decades. Reference 2 provides information about the original design of these tunnels. While multiple collections of blueprints document both major and minor aspects of the construction history, there are few if any validated, archival CAD models that accurately represent the construction history and current geometric details. The recreation of accurate facility models is a tedious task that requires a melding of geometric data and design intent extracted from multiple blueprints, historical reports, and careful physical measurements. Work was started on the creation of an archival, high-fidelity CAD model of the 11-ft TWT in 2011. As questions arose about differences between wind tunnel data and computational results, it became clear that a full model of the tunnel test section leg would allow for vehicles to be analyzed within the environment that they were being tested in. In addition, the facilities engineers at the tunnel recognized that a full computational simulation of the tunnel would be valuable in understanding what could be done to improve the flow characteristics in the test section and make efficient upgrades to the facility. An example of how earlier versions of the tunnel geometry have been used in the past with lower fidelity codes can be found in Reference 3. This report covers the status of the current efforts to accurately model the geometry of the tunnel and simulate the flow within the test section, all in pursuit of a better understanding of the 11-ft TWT and the operation of its main features including the flexible nozzle, slotted walls, model support strut, and diffuser. The limited initial comparisons presented in this report clearly indicate that additional improvements to the geometry model, meshing approach, and boundary condition strategies will be needed to fully meet these goals. Ultimately, the results of these simulations are intended to guide future development of a simplified CFD simulation strategy that can replicate the effects of the tunnel environment on aerodynamic data while eliminating many of the geometry and meshing complications of incorporating the full tunnel geometry.

2.0 GEOMETRY

2.1 Geometry Information Sources

Reconstructing the geometry of the 11-ft TWT for CFD presents an interesting combination of historical and geometric challenges. Because it was designed in the late 1940s, the geometry and construction specifications were done using blueprint drawings. These drawings are available in an Ames archive and have been invaluable for geometric reference during the creation of the CAD models. The CAD geometry model was created using the PTC tools ProEngineer and Creo4. Our current 11-ft TWT model has over 81k surfaces and includes multiple centerbody and model support strut geometries. Special care has been taken to include the outer tunnel plenum walls, bulkheads, and the over 24k baffles in wall slots designed to reduce shock reflections from the test section walls during transonic testing. These slots with baffles perforate the test section walls and allow flow communication between the plenum and the test section to help prevent choking at the model at the higher Mach numbers. The semi-transparent image in Figure 2 shows the current CAD model of the 11-ft TWT test section leg with slotted wall section and surrounding plenum.

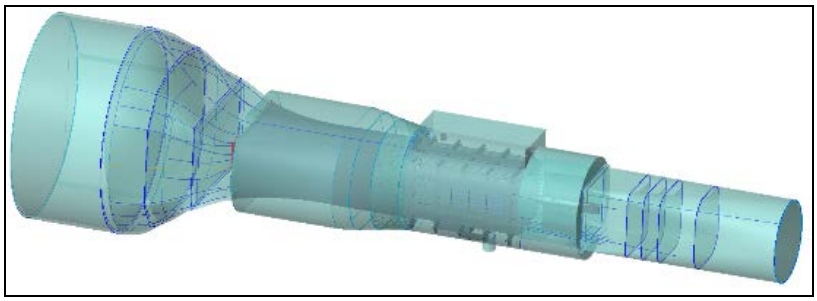

Figure 2: UPWT CAD Model

There were three primary information sources used to create the CAD model. Initially an early (and

undocumented) CAD model of the main tunnel structure in the region of the test section was obtained from the wind tunnel group. This model was created with basic structural analysis in mind, and though it contained much of the primary structure, it did not accurately represent many of the important aerodynamic details of the actual geometry. Original building drawings obtained from onsite archives were the main source of the information and specifications used to create the primary airflow path. These provided enough information to create a model of the test leg that begins just downstream of the 90deg turn and includes the inlet contraction, nozzle flexible walls, test section with slotted walls and surrounding plenum, and most of the aft diffuser. Numerous in-person visits were made to take pictures and take direct measurements of the features of interest. Figure 3 shows photos and images of three geometry details and the resulting CAD geometry representation.

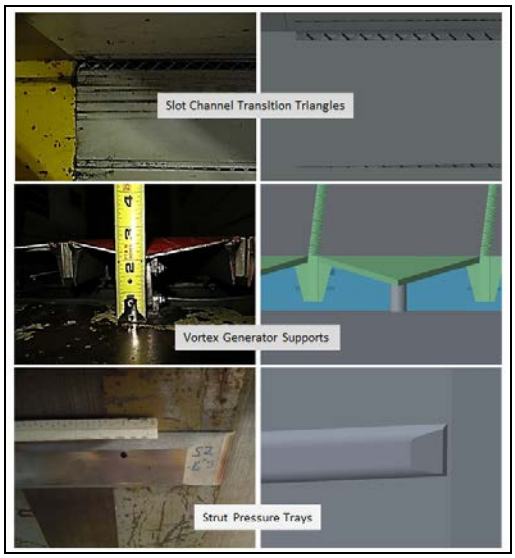

Figure 3: Geometry Modelling Details

Figure 4 shows the axis system at the tunnel origin point (0, 0, 0) in a cutaway view. The figure also shows the various subregions of the geometry that allow for the application of customized surface and volume mesh parameters. Note that while some areas share very similar colors, they are separate regions.

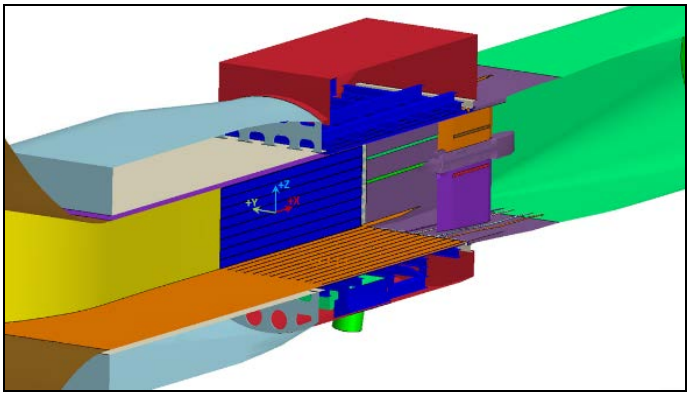

Figure 4: Coordinate System and Surface Region Layout

Reference 5 documents the initial creation of the CAD model. For the analyses described in this paper, additional details were added, and many areas were refined to increase the fidelity of the model.

2.1 Simulation Geometry

The 11-ft TWT surface geometry model was output in STEP format from Creo before being imported into the STAR-CCM+ (Ref. 6) commercial CFD code with integrated meshing, flow solution, reporting, and visualization. STAR-CCM+ has been used in numerous aerospace applications at NASA Ames and excels in meshing complicated internal flow geometries that require subsequent viscous simulation. Partial views of the original CAD geometry along with the STEP format geometry read in to STAR-CCM+, the remeshed surface and finally the volume surface mesh are shown in Figure 5. Numerous combinations of different geometry inputs and volume meshes are being actively investigated as we try to develop tunnel geometry models and volume mesh settings that support the desired fidelity of the simulations. The geometry input definition for the configurations presented in this report contain approximately 620k elements, and the resurfaced meshes contain approximately 8.5M surface elements. The trimmed mesher option in STAR-CCM+ was used to create unstructured hexahedral volume meshes (with prism layers at the walls) containing approximately 60M cells.

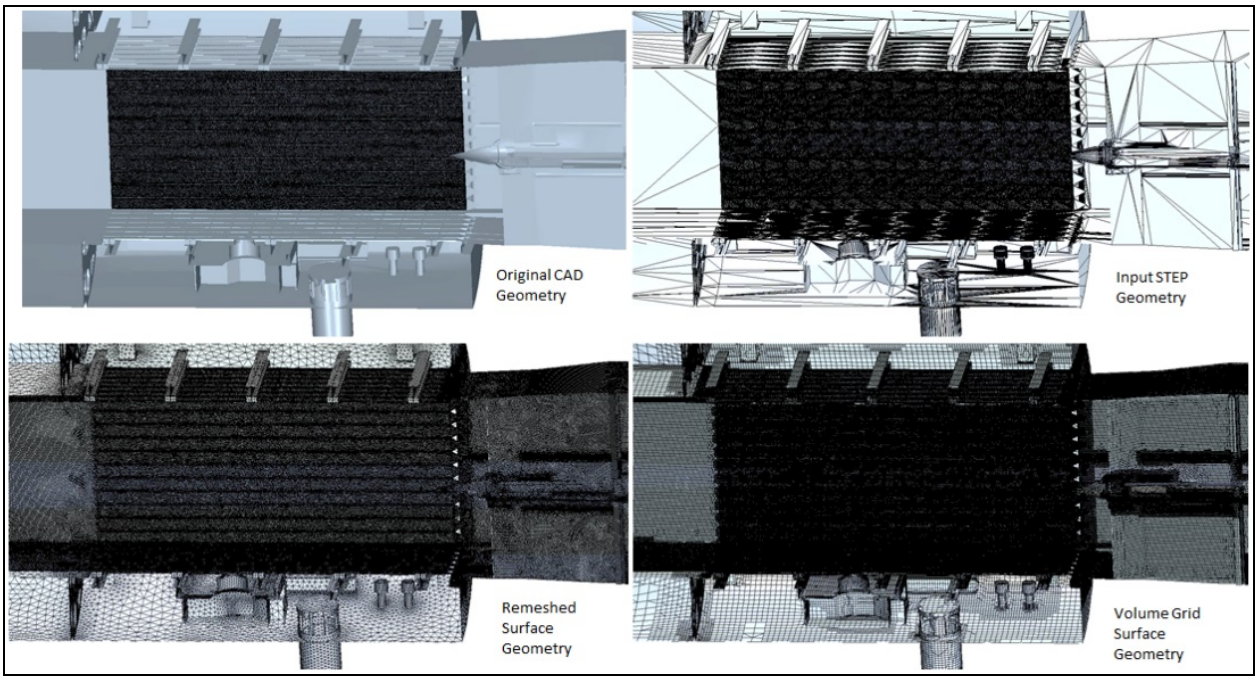

Figure 5: Partial View of Tunnel Geometry, Surface Mesh and Volume Grid

2.2 Simulation Description

The slotted walls of the 11-ft TWT contain over 24,000 small channels that connect the test section to the surrounding plenum. This important ventilation system allows for accurate testing of aircraft and spacecraft at transonic flight conditions but poses a severe challenge to accurate computer simulations as its incorporation requires resolution of geometric details that range in size by over three orders of magnitude.

CFD simulations of the test section leg of the tunnel require careful application of inlet inflow and diffuser outflow boundary conditions, along with simulation of the plenum ventilation system during supersonic operations. Experiments are currently planned to measure 1) the detailed characteristics of the flow exiting the slotted region, 2) the wall pressures at the start of the diffuser, and 3) boundary layer thicknesses in the diffuser downstream of the strut. Once available, these measurements will be used to more accurately set the CFD boundary conditions. Figure 6 below is an image of the 11-ft TWT strut and centerbody taken from a recent CFD simulation of the 11-ft TWT.

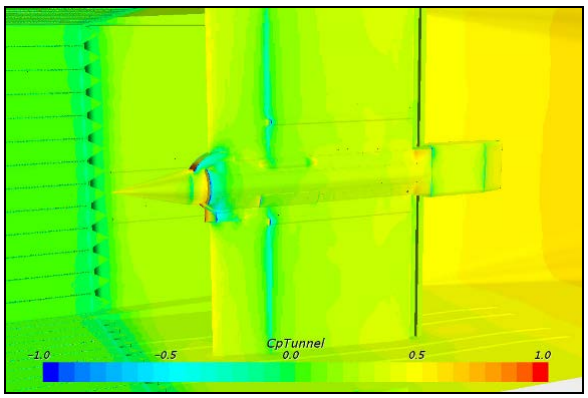

Figure 6: Sample CFD Simulation on 11-ft TWT Strut and Centerbody

2.3 Simulation Status

Over 250 different simulations attempts have been made while studying various combinations of flow solver configurations, surface mesh inputs, volume mesh strategies, and entrance and exit boundary conditions in pursuit of a robust simulation strategy. These simulations were performed for two primary test cases: Mach 0.80 (with undeflected nozzle walls) and Mach 1.2 (with deflected nozzle walls). All simulations assumed adiabatic walls and used the k-ε turbulence model. While there have been at least twelve different volume meshes created, many of them failed when initially attempting to run the flow solver, highlighting both obvious and non-obvious issues that necessitated correction of the underlying geometry. While the geometry of the nozzle's flexible sidewalls is different, the same surface mesh settings and volume grid parameters were used for both the Mach 0.80 and 1.20 cases.

A variety of outputs in addition to the conventional flow solver residuals are continually monitored during the creation of the flow simulations. Figure 7 shows a sample screen image captured while monitoring a typical Mach 0.80 STAR-CCM+ simulation. Shown in this example are plots of the centerline Mach number in the test section, the maximum Mach number both in the full domain and at a specific reference point (125, 0, 0), the mass flows for the inlet, outlet, and their sum, the drag force on the strut and centerbody, and the stagnation pressures and flow velocities at the floor rake locations.

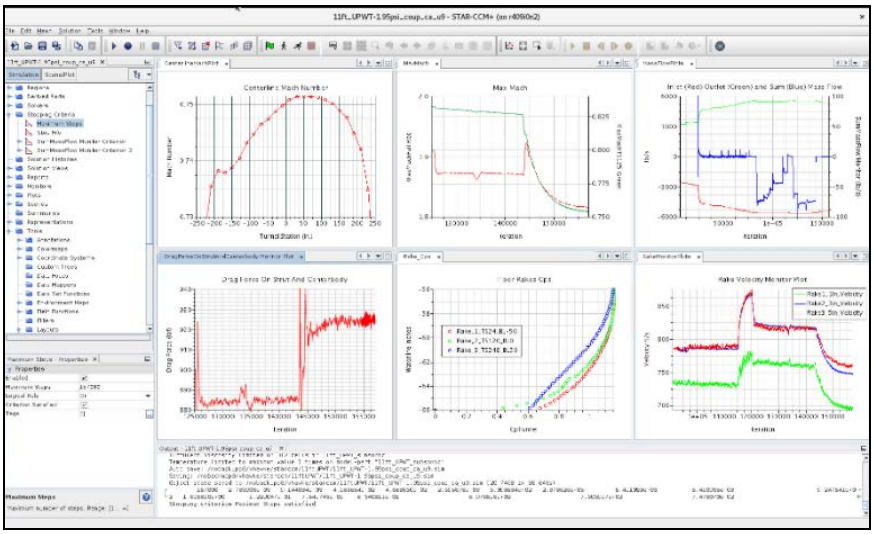

Figure 7: Sample Simulation Monitor Screen

3.0 TUNNEL TESTING

From a facility perspective, developing a validated 11-ft TWT CFD model is driven by the need to run trade

studies of facility modification concepts in CFD prior to pursuing such modifications to the wind tunnel's test section and surrounding plenum, model support systems, and high-speed diffuser. Initial use of the validated CFD model will be to better understand flow conditions in the high-speed diffuser and their effect on the rear model support.

Data were acquired for CFD validation efforts during two tests. The first was performed in March 2014, and the second in May 2017. The first test had the aft diffuser pressure trays installed and included data from the test section wall sensors. The later test provided data for the three boundary layer rakes on the floor of the test section, positioned as shown in Figure 8. The testing described in this report was performed at sub-sonic, transonic and super-sonic conditions at atmospheric pressure. A future test to acquire additional diffuser data is in the preliminary planning stages.

4.0 CFD RESULTS AND COMPARISONS TO TEST DATA

As mentioned in section 3 above, the pressure data forcomes from two separate tests. Two conditions were chosen for the comparisons of the CFD simulations and experimental data. Mach 0.80 is a common speed at which transport aircraft are tested in the tunnel and Mach 1.2 is often a test point for supersonic fighter jets. There are many figures of merit that were monitored while the simulations advanced, including direct comparisons to several different sets of tunnel measurements. Figure 8 shows the locations of the various test instrumentation sets including four of the eight test section wall static pressure tap rows, the aft diffuser pressure trays, two of the four strut pressure trays and the boundary layer rakes on the test section floor. The dimensions in the image are in inches. Additional comparisons are also shown using the centerline static pressure data that was taken in earlier empty tunnel calibration tests.

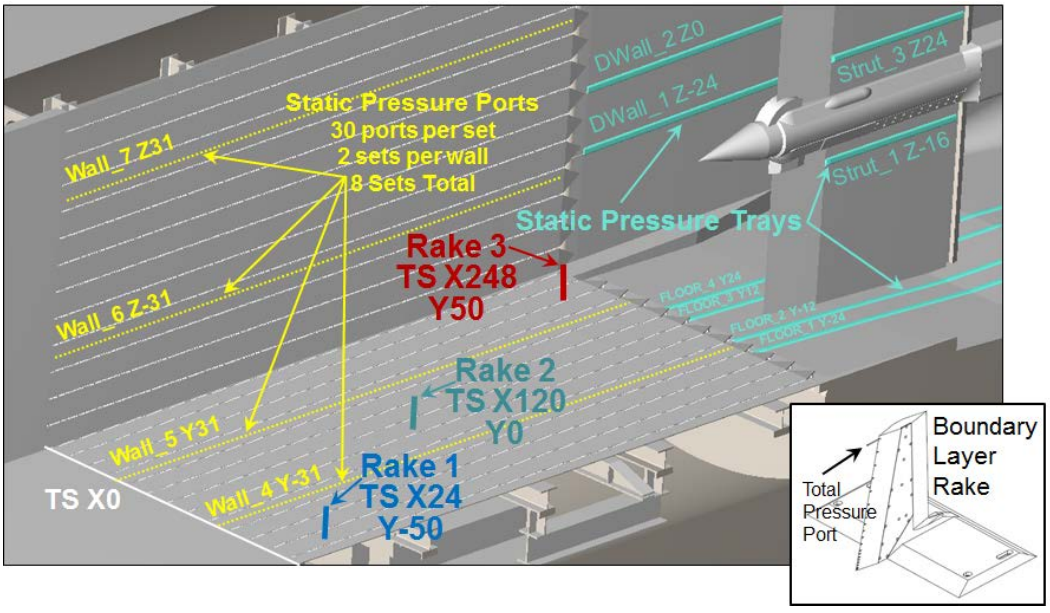

Figure 8: Location of Test Instrumentation for CFD Validation Tests

The data being presented should be interpreted as a snapshot of the current simulation strategy. While the results are approaching the desired level of fidelity from the model, they each have some aspects that will require more work. In addition to the direct comparison of the results to the tunnel data, other aspects of the solution were examined to determine how well it modelled the actual measured tunnel flow. This included the overall homogeneity of the flow in the test section, the state of the flow in the aft diffuser and the overall stability of the solution. Both solutions presented conserve mass flow through the full tunnel. There are many aspects to modelling the full tunnel flow accurately that will ultimately require additional tunnel data

to help improve the simulation accuracy. While attempting to achieve the desired flow speeds, it became clear that some of the complex interplays between the plenum and tunnel test leg free-stream flow characteristics are not well understood. One of the areas of uncertainty is located near the forward leading edge of the diffuser transition and the aft test section vortex generators, both of which affect the flow between the plenum chamber and the main flow path. Another item of uncertainty is the amount of blockage created by objects like cameras and other instrumentation that reside behind the test section tunnel walls (and are not accounted for in the geometry modelling due to their temporary installations). While every attempt has been made to include the primary permanent features of the tunnel in the model, there remain many items that could likely affect the overall flow pattern in and out of the plenum chamber. Yet another source of difference between the model and the actual tunnel is in the area of the inlet nozzle. Although care was taken to parameterize the shape of the flexible walls based on the design specification, a detailed scan of the actual wall positions will be needed to ensure that the model does in fact represent the actual tunnel properly, especially during supersonic operation. Another issue with the modelling of the tunnel flow is the condition of the flow in the aft diffuser. Little is known about the actual thickness of the boundary layer aft of the strut and the actual flow velocity and uniformity at the downstream turn/outlet.

There are several known differences between the physical and simulated tunnel configurations. During the test that produced the rake data, the strut centerbody was located at its uppermost position (which positions the centerbody near the tunnel ceiling). The data shown below has the tunnel configured with the centerbody at the centerline or Z = 0 position. This difference is not expected to have much if any effect on the results in the test section, and it enabled a single configuration to be run in the simulation that reflected the position during the testing when the aft diffuser and test section wall pressures were measured.

The pressure coefficient values were calculated in the same manner for both the tunnel test and the simulation, using reference values extracted from a fixed reference point in the tunnel. For this work, Cp, as shown on the charts, and Cp Tunnel, as used in the simulation, are synonymous, and are both measurements of stagnation pressure. The reference point is located at tunnel station 168 (inches) on the centerline (168,0,0). Reference values for density, velocity magnitude, total pressure, and static pressure were extracted from the simulations at the same reference point and used in the Cp calculation as follows:

$$\text{RefPressureTS168} = \text{AbsoluteTotalPressureTS168} + \text{StaticPressureTS168}$$

$$\text{QRefTS168} = (\text{DensityTS168} * \text{VelocityTS168}^2) / 2$$

$$C_p \text{ Tunnel} = (\text{AbsoluteTotalPressure} - \text{RefPressureTS168}) / \text{QRefTS168}$$

4.1 Target Mach 0.80

For the Mach 0.80 case, the coupled flow solver provided the most satisfactory comparisons. Figure 9 shows the centerline Mach number comparison for this case. The pressure coefficients for the three test section floor boundary layer rakes are given in Figure 10. Figure 11 shows comparisons with the wall static pressure coefficient data. Figure 12 provides the comparisons for the aft diffuser and Figure 13 shows the Cp distributions for the pressure trays on the strut.

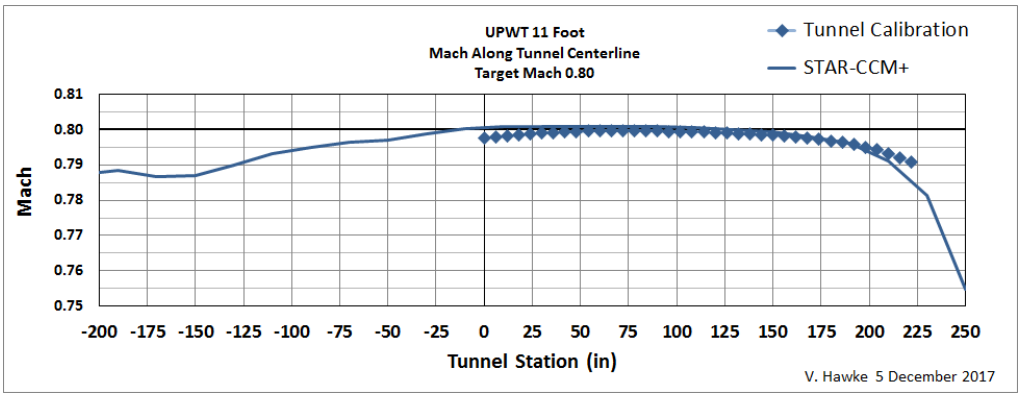

Figure 9: Mach 0.80 Centerline Mach Number

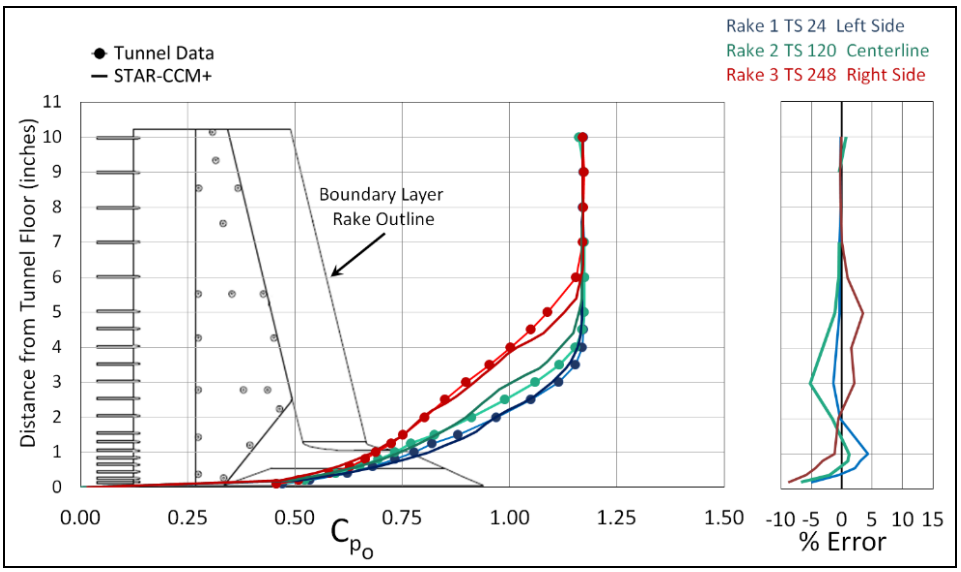

Figure 10: Mach 0.80 Boundary Layer Rake Pressures

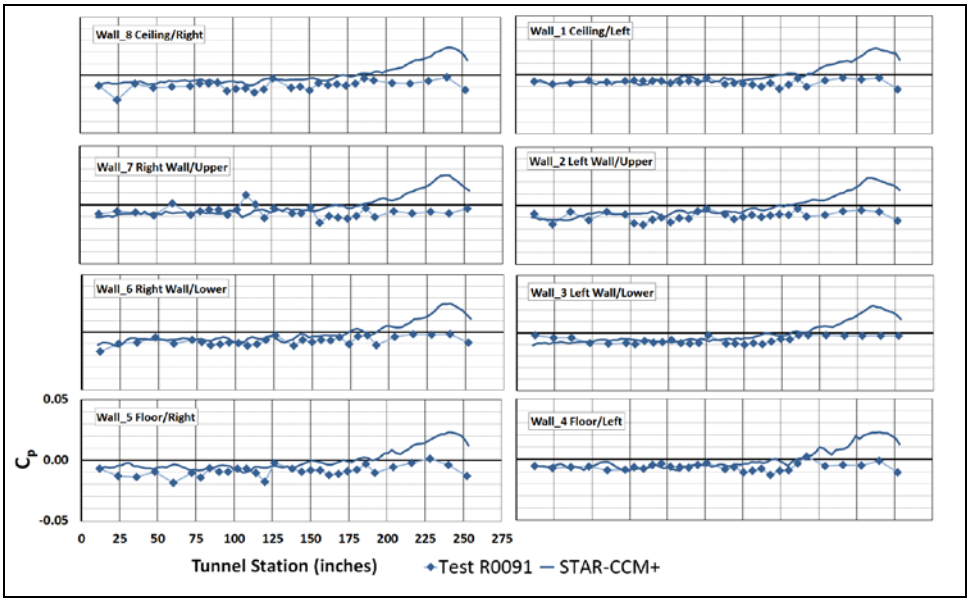

Figure 11: Mach 0.80 Test Section Wall Static Pressure Distribution

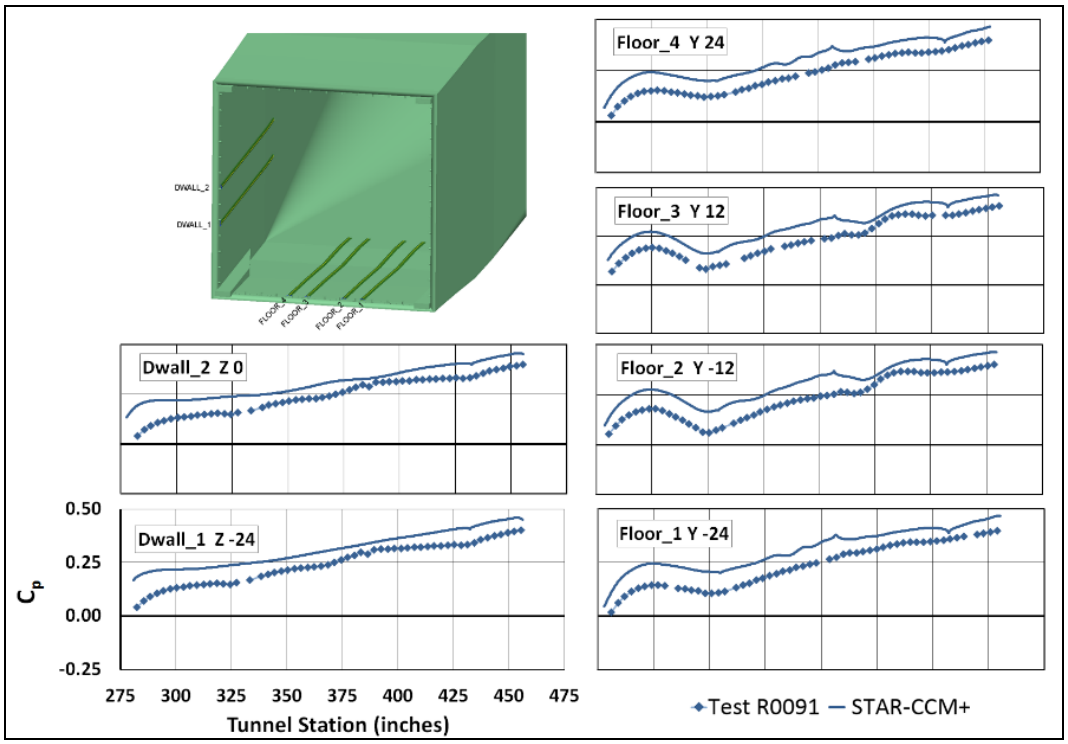

Figure 12: Aft Diffuser Floor and Wall Static Pressure Distributions

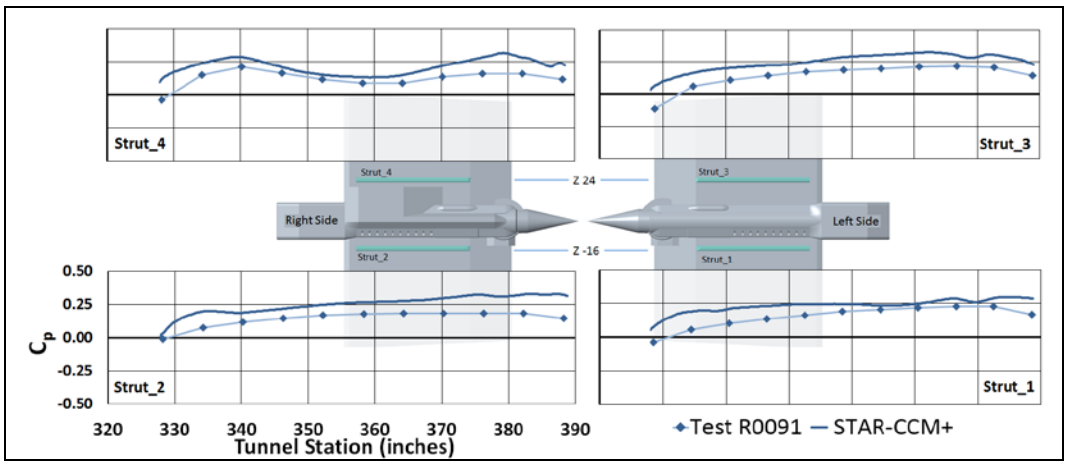

Figure 13: Static Pressure Distributions For Aft Diffuser Strut Pressure Trays

It is not fully understood why the wall pressures rise near the end of the test section in the STAR-CCM+ simulation, however it could be related to the amount of flow being reentrained from the plenum chamber in to the main flow. A view of the flow from the plenum chamber through the aft test section vortex generators is shown in Figure 14.

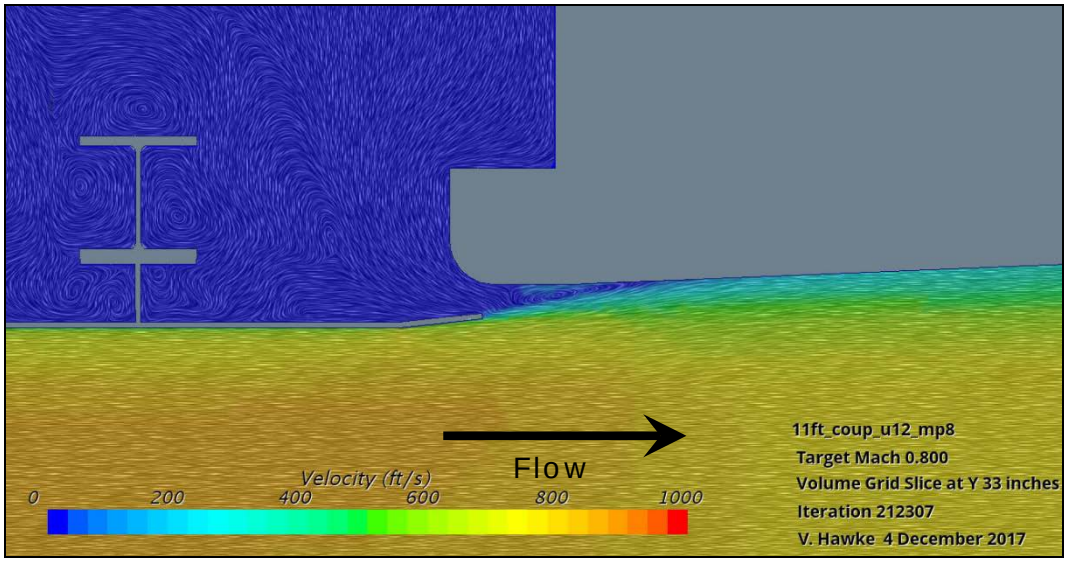

Figure 14: Mach 0.80 Flow from Upper Plenum Chamber in to Test Section

4.2 Target Mach 1.2

For the Mach 1.2 case, the segregated flow solver provided the most satisfactory comparisons. Figure 15 shows the centerline comparison for the Mach 1.2 case. The pressure coefficients for the three test section floor boundary layer rakes are given in Figure 16. Figure 17 shows comparisons with the wall pressure data. Figure 18 provides the comparisons for the aft diffuser and Figure 19 is for the pressure trays on the strut.

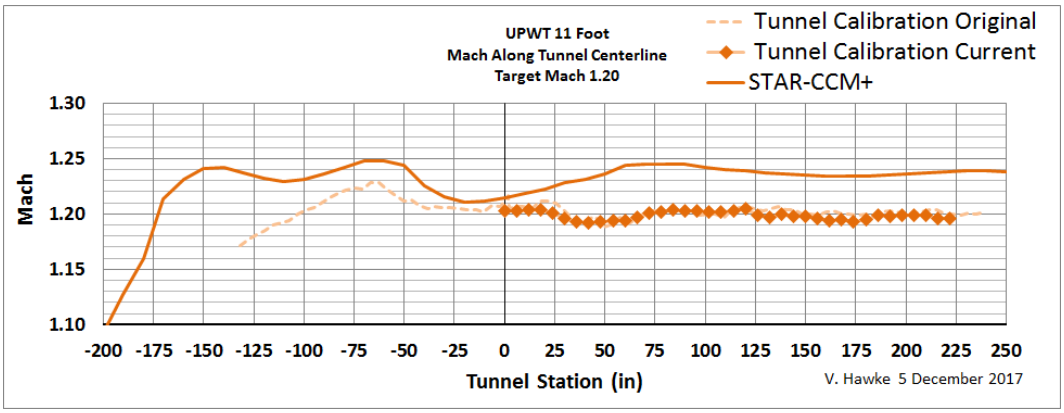

Figure 15: Mach 1.2 Tunnel Centerline Mach Number

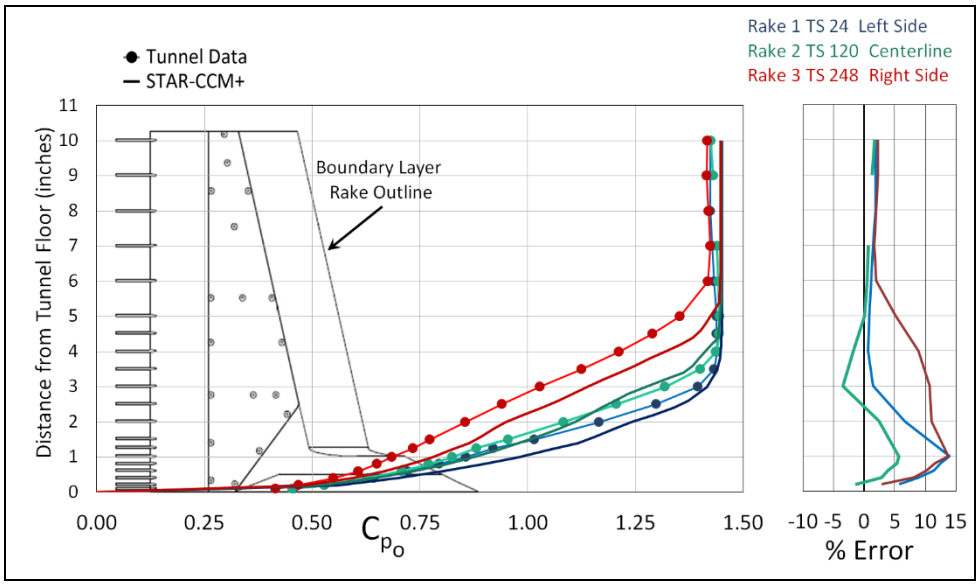

Figure 16: Mach 1.2 Test Section Boundary Layer Rake Pressures

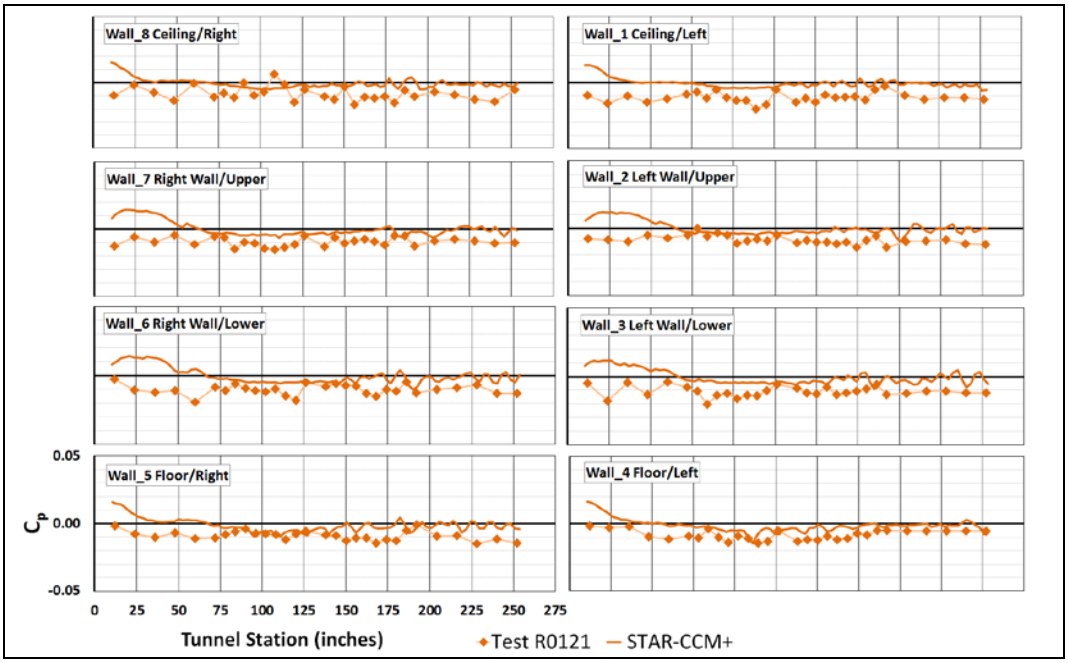

Figure 17: Mach 1.2 Test Section Wall Pressure Distributions

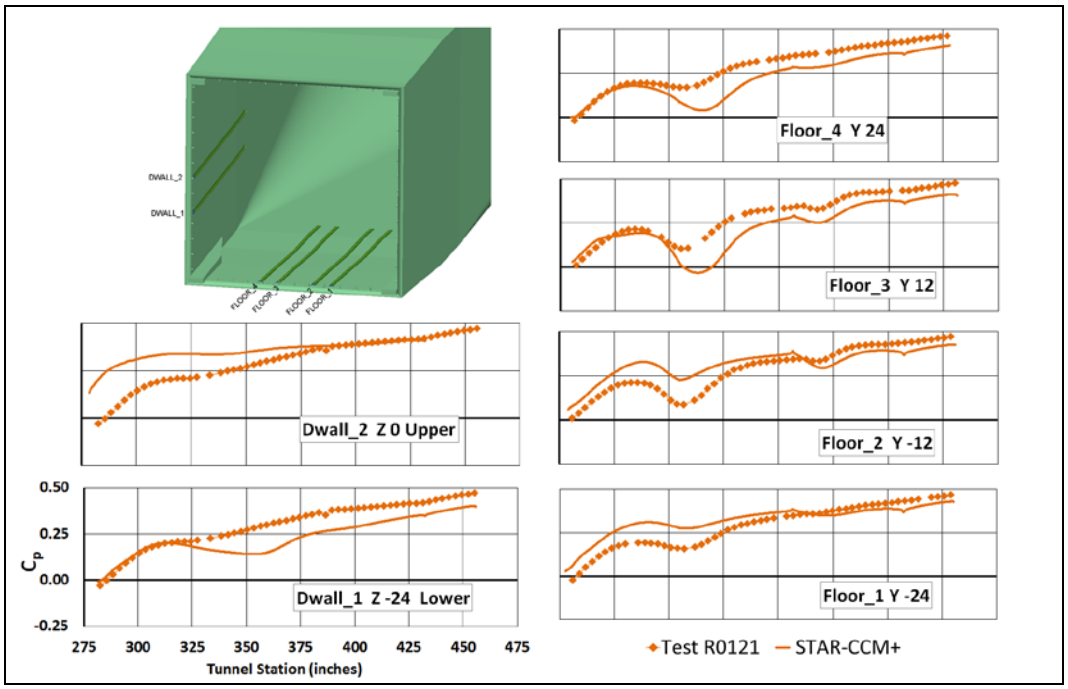

Figure 18: Mach 1.2 Aft Diffuser Pressure Distributions

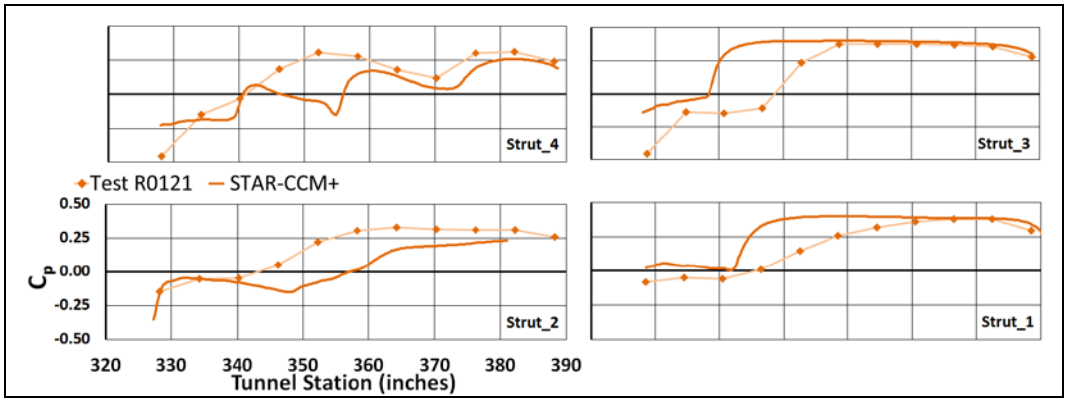

Figure 19: Aft Diffuser Strut Pressure Distributions

It is clearly apparent in Figure 15 that the centerline Mach number from the CFD simulation for this case is higher than the experimental Mach 1.2 data, producing a slight offset in the overall level of the wall and strut pressure distributions. This is most likely due to an inaccuracy in reproducing the nozzle wall deflections. The solution was still considered reasonable since the shape of the aft diffuser pressure profiles matched well with the test data. Work was done on determining the correct boundary mass flow to use in the plenum evacuation system (mass pump). The mass pump is an auxiliary compressor which can operate up to 50,000 cfm and is sometimes used to pump out air to help bleed off the boundary layer through the test section slots at higher Mach numbers. Without further information about the actual flow through the pump it was decided to run the case with the pump exit velocity set to zero, since from test notes it seems likely that the pump was not used for all Mach 1.2 cases. Further running of the simulation with additional tunnel information would likely allow for the solution to more closely match the test data.

The diffuser flow for this case appears to have a substantial region of nearly sonic flow with a terminal shock system positioned just downstream of the test section exit. Stabilizing the flow such that terminal shocks stayed clear of the vortex generators (where the plenum chamber flow is re-entrained) proved to be rather challenging. Without details about what the downstream pressures were expected to be, the thickness of the boundary layer in the aft diffuser, and the state of the plenum mass pump flow, producing stable simulations was a balancing act. Figure 20 shows a cross section of the flow at a constant Y of +21 inches between the strut and tunnel walls. It also includes the mass pump in the lower plenum chamber and shows the flow accelerating in the exit diffuser and shocking down to subsonic speed.

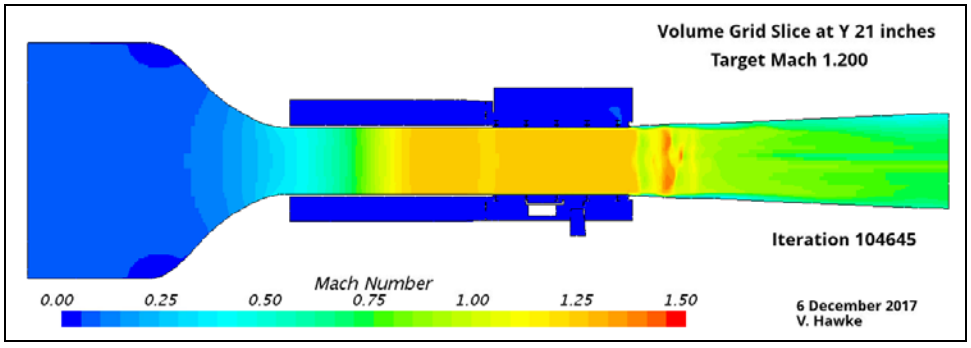

Figure 20: Mach 1.2 Constant Y = 21 Slice

A close-up view of the flow from the plenum chamber through the aft test section vortex generators is shown in Figure 21. A weak flow expansion shock can be seen emanating from the upper surface of the canted vortex generator. These visualizations lead to a better understanding of the flow field in the tunnel and further informs us of where additional instrumentation can help to improve the simulations. This in turn will allow for updates in the tunnel that promote smoother flow and more accurate test results. The same line

integral convolution flow visualization technique used in Figure 21 helps to visualize an area near tunnel station 0 on a waterline cut through a slot channel, and is shown in Figure 22. Note that the line integral convolution fails to resolve in the areas where the mesh density is low and boxed in by geometry resulting in blank spots in the image. Figure 23 shows the volume grid in this area. Better resolution of the volume grid with additional prism layers in the slot channels would improve the visualization of the flow and resolution of the flow details. This is an example of a deficiency that we plan to address in future simulations. Doing so will likely improve agreement with the wind tunnel data.

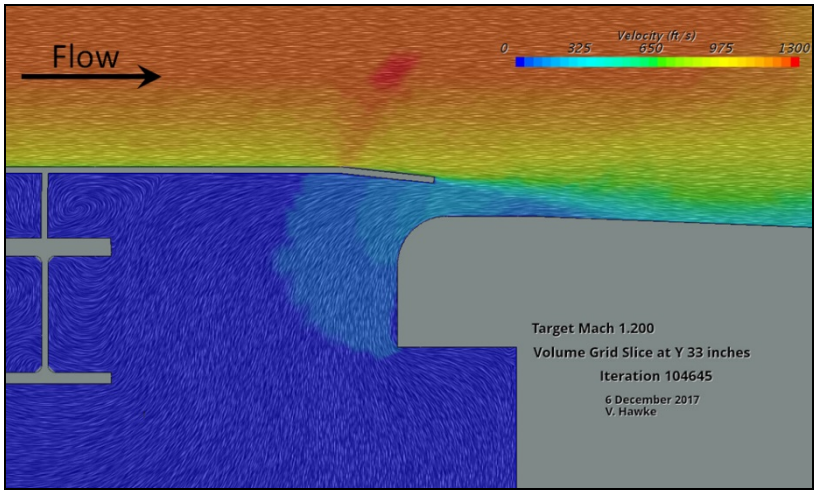

Figure 21: Mach 1.2 Flow Through Vortex Generators

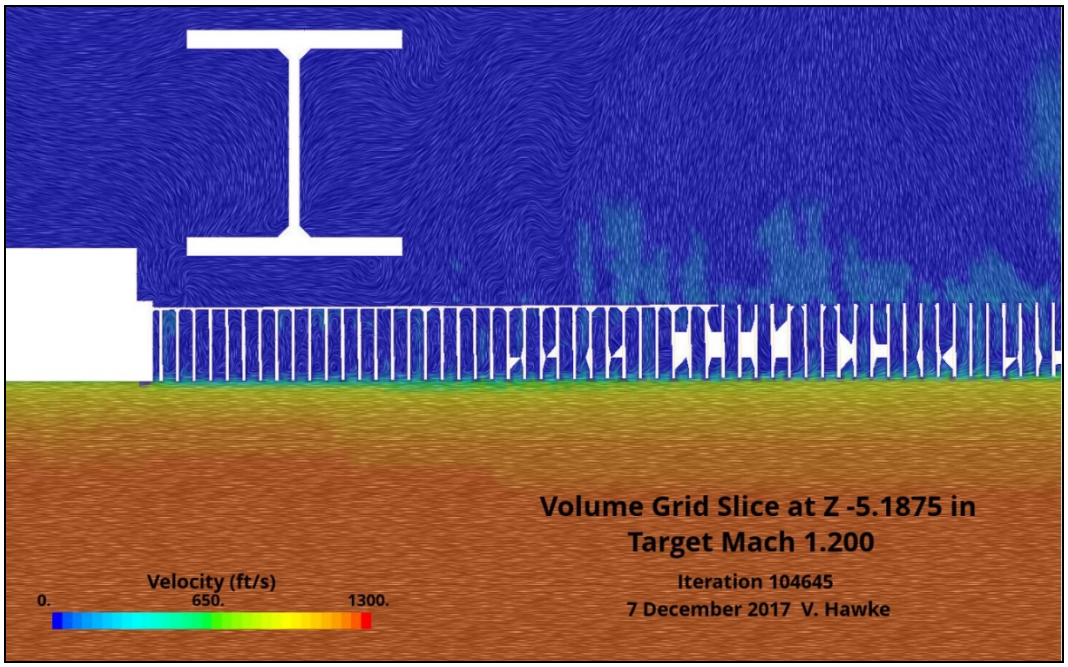

Figure 22: Flow Through Slot Channels at Forward Test Section

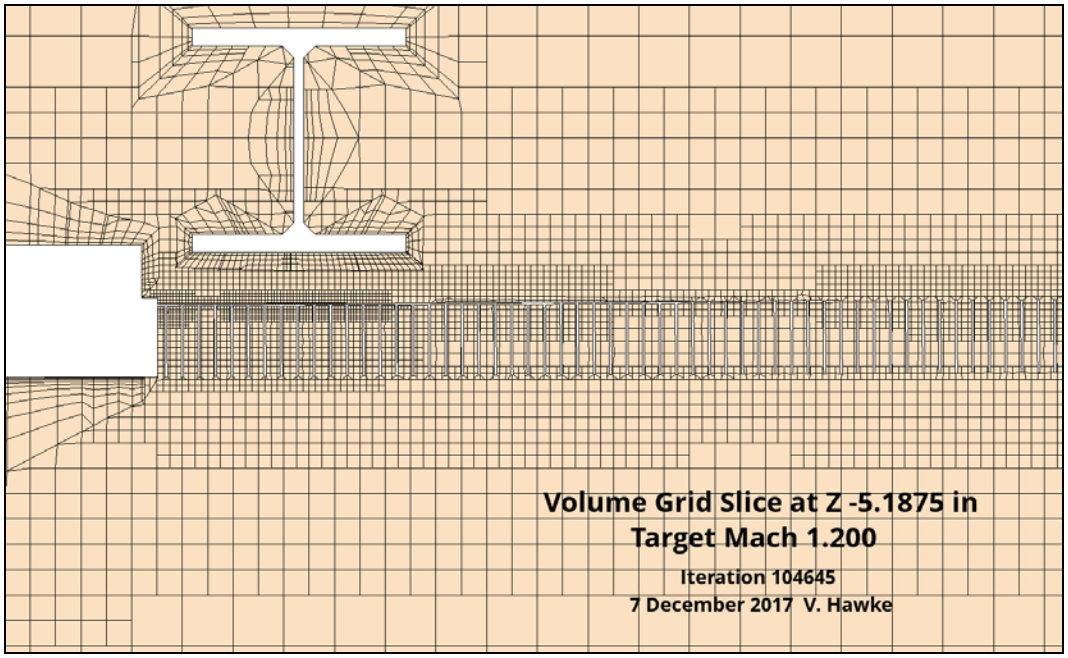

Figure 23: Volume Grid for Slot Channels at Forward Test Section

5.0 CONCLUSIONS

We have shared our recent experiences, both positive and negative, with CFD simulations of the 11-ft TWT and initial comparisons with experimental data taken during wind tunnel tests. This work should be viewed as an encouraging first step towards routine high-fidelity CFD analyses that incorporate highly detailed CAD models of both subject model and the surrounding wind tunnel walls. The fidelity of future simulations will ultimately require further validation data that provides additional insight into tunnel physics and boundary conditions. The transition region between the test section and aft diffuser and the far aft diffuser wall boundary layer and diffuser exit flow face are critical areas where additional measurements could provide the information needed to better understand and simulate the tunnel flow.

REFERENCES

[1] https://www.nasa.gov/centers/ames/orgs/aeronautics/windtunnels/11x11-wind-tunnel.html

[2] Huntsberger, R. F. and Parsons, J. F. (1954) The Design of Large High-Speed Wind Tunnels, AGARD Forth General Assembly, Scheveningen, Netherlands.

[3] Hawke, V. M. (2015) 11 Foot Unitary Plan Tunnel Facility Optical Improvement Large Window Analysis,
NASA/CR--2015-218481.

[4] PTC, Retrieved from https://www.ptc.com/en/products/cad/pro-engineer

[5] Hawke, V. M. (2014). 11-by 11-Foot Transonic Leg of the Unitary Plan Wind Tunnel (UPWT) CAD Model.
NASA/CR--2014-218371.

[6] STAR-CCM+, Retrieved from https://mdx.plm.automation.siemens.com/star-ccm-plus